Acta Cryst. (1997). B53, 159–167

Isothermal Compressibility and Pressure Dependence of the Crystal Structures of the Superconducting Charge-Transfer Salt κ-(BEDT-TTF)$_2$Cu(NCS)$_2$ [BEDT-TTF = Bis(ethylenedithio)tetrathiafulvalene]

MARIAM RAHAL,[a] DANIEL CHASSEAU,[a]* JACQUES GAULTIER,[a] LAURENT DUCASSE,[b] MOHAMEDALLY KURMOO[c] AND PETER DAY[c]

[a]*Laboratoire de Cristallographie, et de Physique Cristalline Université Bordeaux I, 351 Cours de la Libération, 33405 Talence CEDEX, France,* [b] *Laboratoire de Physico-Chimie Théorique, Université Bordeaux I, 351 Cours de la Libération, 33405 Talence CEDEX, France, and* [c]*The Royal Institution of Great Britain, 21 Albemarle Street, London W1X 4BS, England. E-mail: chasseau@zita.cristal.u-bordeaux.fr*

(Received 1 July 1994; accepted 30 August 1996)

Abstract

From the pressure dependence of the lattice parameters measured by single-crystal X-ray diffraction at room temperature, the amplitudes and directions of the principal components of the isothermal compressibility tensor of κ-(BEDT-TTF)$_2$Cu(NCS)$_2$, bis(ethylenedithio)tetrathiafulvalene copper dithiocyanate, have been determined from 1×10^5 Pa to 12.9×10^5 kPa. The crystal structure has been determined at 1×10^5 Pa and 7.5×10^5 kPa. From the latter, the pressure dependence of the intermolecular electron-transfer integrals and the band structure have been calculated and compared with those at 1×10^5 Pa and 15 K.

1. Introduction

The family of charge-transfer salts based on the electron donor molecule bis(ethylenedithio)tetrathiafulvalene (BEDT-TTF) is notable both for containing the molecular-based superconductors with the highest critical temperature, T_c, presently known, and for the existence of a remarkable number of polymorphic phases (see *e.g.* Williams *et al.*, 1992). The superconductors with the highest T_c's in this group belong to the so-called κ-phase. Being molecular in nature, the crystals of these compounds are relatively compressible and it has been of interest to observe how the physical properties evolve as a function of hydrostatic pressure. Under these circumstances there is not only a variation in the intermolecular electronic transfer integrals that determine the band structure, but the possibility of structural or electronic phase transitions that may lead to drastic changes in physical properties. For example, among the superconducting BEDT-TTF charge-transfer salts, T_c decreases with increasing pressure, except for β-(BEDT-TTF)$_2$I$_3$ [T_c at ambient pressure 1.5 K (Yagubskii *et al.*, 1984)], which exhibits a sharp transition at 1×10^5 kPa to a phase labelled β_H- with T_c around 7–8 K (*e.g.* Tokumoto *et al.*, 1990; Tokumoto *et al.*, 1985).

The salt κ-(BEDT-TTF)$_2$Cu(NCS)$_2$ has one of the highest ambient pressure T_c's known among charge-transfer salts (10.4 K; Urayama, Yamochi, Saito, Nozawa *et al.*, 1988), but above 6×10^5 kPa T_c is reduced to zero. There has been some controversy regarding the precise form of the pressure dependence of T_c. Parker *et al.* (1989) found T_c approximately invariant up to $\sim 3 \times 10^5$ kPa, followed by a rapid fall, while Kang, Jerome, Lenoir & Batail (1990), Tokumoto *et al.* (1990), Schirber *et al.* (1988) and Caulfied *et al.* (1994) reported an approximately linear decrease. More recently Fujii *et al.* (1993) have found behaviour similar to that reported by Parker *et al.* (1989). It has also been shown that the frequency of Schubnikov de Haas oscillations in the magnetoresistance varies with pressure, indicating a variation in the band structure (Oshima *et al.*, 1988; Lubczynski *et al.*, 1994). Finally, the pressure dependence of the normal state conductivity of κ-(BEDT-TTF)$_2$Cu(NCS)$_2$ is also somewhat unusual as is its variation with temperature. At ambient pressure the resistance at first increases on cooling from 300 K to reach a maximum of $\sim$100 K, below which it falls in the usual way characteristic of a metal. On applying hydrostatic pressure the resistivity maximum is progressively suppressed until at 5×10^5 kPa the resistance shows a monotonic decrease continuously from 300 K down to T_c. At 300 K the resistivity is decreased by a factor of 4 on applying 5×10^5 kPa (Parker *et al.*, 1989).

In view of the observed effects of pressure on both the superconducting and normal state properties, it is clearly important to determine the pressure dependence of the crystal structure of κ-(BEDT-TTF)$_2$Cu(NCS)$_2$. In this paper we report the ambient temperature crystal structure at 1×10^5 Pa and 7.5×10^5 kPa together with the amplitudes and directions of the principal components of the isothermal compressibility tensor. From the crystal structure, the electronic band structure has been

calculated at 1×10^5 Pa and 7.5×10^5 kPa. A preliminary account of part of this work has been given (Chasseau *et al.*, 1991). Comparison is made with similar calculations at 15, 104 and 295 K and ambient pressure.

2. Experimental

2.1. *Synthesis and crystal growth*

BEDT-TTF was synthesized by the method of Larsen & Lenoir (1988) and recrystallized twice from chloroform. Crystals of κ-(BEDT-TTF)$_2$Cu(NCS)$_2$ were grown electrochemically on a platinum electrode at constant current (1.5 μA) from a solution of 1,1,2-trichloroethane (90%) and ethanol (10%), both of which had been purified by distillation. The source of the anion was a stoichiometric mixture of CuSCN, KSCN and 18-crown-6 ether and the crystallization process lasted 2 weeks. The crystals were in the form of thin plates, typically $1 \times 0.5 \times 0.05$ mm.

2.2. *Pressure cell*

The high-pressure cell constructed at the University of Bordeaux consists of a cylindrical hard steel frame 40 mm in diameter and 40 mm high made from two plates joined by three pillars at 120°. Two cone-shaped diamond anvils, each of 0.25 carat, are fixed to hard steel supports, one of which is secured to the frame while the other can be moved. The diamond anvils press on a 0.5 mm thick Be disc of diameter 3 mm, pierced by a 0.3 mm diameter cylindrical hole that makes up the high-pressure enclosure, inside which are the sample, the pressure transmitting fluid (fluorinert: C_6F_6) and a pressure sensor. The latter consists of a thin sublimed film of bis(dimethylglyoximato)nickel, which has an optical absorption band in the visible region whose wavelength varies linearly with pressure up to at least 35×10^5 kPa. The final adjustment of the faces of the anvils is made under a microscope, to ensure that they are parallel and that the hole in the Be disc is precisely centred. The crystal to be studied is cut normal to its longest direction in such a way that its height is less than the thickness of the Be disc: it is then placed on that face onto the surface of the diamond, to which it is first attached by an extremely thin layer of silicone oil. The cell is designed to be used either with precession or Weissenberg cameras or with inclination diffractometers.

2.3. *Cell parameters*

The crystal cell constants were determined as a function of pressure up to 13×10^5 kPa from 20 intense reflections ($14 < \theta < 34°$) selected from preliminary Weissenberg photographs. The measurements were carried out using an AED-Siemens automatic diffractometer operating in equatorial geometry using Cu $K\alpha$ radiation ($\lambda = 1.5418$ Å), by determining the three Euler angles (θ, χ, φ) of each reflection. The cell parameters were refined from these data by the least-squares method.

2.4. *Crystal structure determination*

Exploration of reciprocal space and intensity measurements were made using a STOE automatic equi-inclination diffractometer. The X-ray radiation was graphite-monochromatized Mo $K\alpha$ (0.70926–0.71354 Å) from a rotating anode generator. Intensities were measured by the ω-scan method. Efficient collimation reduced scattering from the Be and diamond, nevertheless, the background was high and inhomogeneous. The profile of each reflection was, therefore, examined on a graphics screen in order to choose the optimum baseline and integrated intensity using the local program *PROFIL* (Loumrhari, 1983).

The crystal used for the pressure study was twinned, but observation of the profiles of individual reflections indicated that the large majority of the resulting pairs of reflections were well separated. Those that were not were excluded from the refinement.

The Ahmed–Marsau suite of programs was used to refine the structure by the block-diagonal least-squares method. Starting parameters were taken from Urayama, Yamochi, Saito, Sato *et al.* (1988). Crystal data at 1×10^5 Pa and 7.5×10^5 kPa are listed in Table 1.

3. Results and discussion

3.1. *Isothermal compressibility*

At ambient pressure κ-(BEDT-TTF)$_2$Cu(NCS)$_2$ crystallizes in the monoclinic system $P2_1$ (Urayama, Yamochi, Saito, Sato *et al.*, 1988). The unit-cell constants were determined at eight pressures between 1×10^5 Pa and 12.9×10^5 kPa, because the ω profiles of the reflections broadened noticeably above 13×10^5 kPa. In each measurement the same group of reflections was used and the pressure was determined with the crystal *in situ* by the method described above. The values of the cell constants are listed in Table 2. No singularity is observed in their variation over the whole range of pressures, which can be parametrized in terms of second degree polynomials by least-squares fitting ($x = l + mP + nP^2$). The fitted values of l, m and n are listed in Table 3, from which it can be seen that the decrease in the cell lengths is almost a linear function of pressure over this range. Overall, it appears that the lattice of κ-(BEDT-TTF)$_2$Cu(NCS)$_2$ is less compressible than those of other related compounds: for example, $(I/V)(dV/dP) \times 10^8$ kPa^{-1} is 6.5 compared with 7.5 in (TMTSF)$_2$ClO$_4$ (Houbib, 1988), 8.0 in (TMTSF)$_2$PF$_6$ (Gallois, Gaultier, Hauw, Lamcharfi

Table 1. *Experimental details*

	1×10^5 Pa	7.5×10^5 kPa
Crystal data		
Chemical formula	$2C_{10}H_8S_8.Cu(NCS)_2$	$2C_{10}H_8S_8.Cu(NCS)_2$
Chemical formula weight	949	949
Cell setting	Monoclinic	Monoclinic
Space group	$P2_1$	$P2_1$
a (Å)	16.228 (5)	16.138 (3)
b (Å)	8.442 (4)	8.300 (1)
c (Å)	13.113 (4)	12.829 (3)
β (°)	110.26 (1)	111.27 (2)
V (Å^3)	1685	1601
Z	2	2
D_x (Mg m^{-3})	1.87	1.97
Radiation type	Mo $K\alpha$	Mo $K\alpha$
Wavelength (Å)	0.71073	0.71073
No. of reflections for cell parameters	20	20
θ range (°)	14–34	14–34
μ (mm^{-1})	1.91	2.01
Temperature (K)	295	295
Crystal form	Plate	Plate
Crystal size (mm)	$1.0 \times 0.5 \times 0.05$	$1.0 \times 0.5 \times 0.05$
Crystal colour	Black	Black
Data collection		
Diffractometer	Stoe Stadi-2 Equi-inclination	Stoe Stadi-2 Equi-inclination
Data collection method	ω scans	ω scans
Absorption correction	None	None
No. of measured reflections	3784	2582
No. of independent reflections	3784	2582
No. of observed reflections	3388	1741
Criterion for observed reflections	$I > 2\sigma(I)$	$I > 2\sigma(I)$
θ_{max} (°)	25	25
Range of h, k, l	$0 \rightarrow h \rightarrow 20$ $0 \rightarrow k \rightarrow 8$ $-20 \rightarrow l \rightarrow 20$	$0 \rightarrow h \rightarrow 20$ $0 \rightarrow k \rightarrow 7$ $-20 \rightarrow l \rightarrow 20$
No. of standard reflections	2	2
Frequency of standard reflections	Every 50 reflections	Every 50 reflections
Refinement		
Refinement on	F	F
R	0.051	0.098
wR	0.060	0.052
S	1.0	2.4
No. of reflections used in refinement	3388	1741
No. of parameters used	396	275
H-atom treatment	H-atom parameters not refined	H-atom parameters not refined
Weighting scheme	$w = 1/\sigma^2(F)$	Robust-resistant weighting scheme used
$(\Delta/\sigma)_{max}$	0.0005	0.0016
$\Delta\rho_{max}$ (e Å^{-3})	0.4	1.1
$\Delta\rho_{min}$ (e Å^{-3})	−0.3	−0.5
Extinction method	None	None
Source of atomic scattering factors	*International Tables for X-ray Crystallography* (1974, Vol. IV) and Cromer & Waber (1974)	*International Tables for X-ray Crystallography* (1974, Vol. IV) and Cromer & Mann (1968)

& Filhol, 1986) and 8.2 in α'-(BEDT-TTF)$_2$AuBr$_2$ (Chasseau *et al.*, 1993). However, it is a matter of great interest that the variation of the cell constants with pressure is quite different from that observed on lowering the temperature. Table 4 compares the relative decrease in the unit-cell constants and volume on passing from 1×10^5 Pa to 12.9×10^5 kPa at 300 K with those found on lowering the temperature to 15 K at 1×10^5 Pa (Schultz *et al.*, 1991). Especially noteworthy in the latter case was the relative *increase* in a, *i.e.* the direction normal to the BEDT-TTF layers, a result also found for β-(BEDT-TTF)$_2$I$_2$Br (Emge *et al.*, 1986). Clearly the molecular reorganizations brought about by independently changing the two intensive thermodynamic variables of T and P are not at all comparable, a fact that must be taken into account when assessing the influence of these two variables on the physical properties.

From the data in Table 2, the linear compressibilities $[k_x = -(1/x)(dx/dP)]$ are calculated for the three crystallographic directions a, b and c. The variation of k_x with pressure is shown in Fig. 1, from which it can be seen that the compressibility is highly anisotropic (note especially the small value of k_a) and also that all three values vary more or less linearly with pressure. Extrapolating to higher pressure it appears that k_b and k_c would become equal at $\sim 18 \times 10^5$ kPa. It is interesting to note that this is

Table 2. *Unit-cell parameters and volume of κ-(BEDT-TTF)$_2$Cu(NCS)$_2$ as a function of pressure*

At low pressures the e.s.d.'s are 0.005, 0.004 and 0.004 Å for a, b and c, and 0.01° for β; at high pressure they are slightly higher.

P ($\times 10^5$ kPa)	a (Å)	b (Å)	c (Å)	β (°)	V (Å^3)
10^{-3}	16.228	8.442	13.113	110.26	1685
2.8	16.170	8.368	12.962	110.73	1640
6.8	16.109	8.288	12.810	111.16	1595
7.5	16.138	8.300	12.829	111.27	1601
9.7	16.097	8.264	12.719	111.58	1573
10.7	16.083	8.233	12.681	111.67	1560
11.7	16.069	8.225	12.652	111.72	1553
12.9	16.062	8.193	12.637	111.82	1544

Table 3. *Pressure variation of unit-cell parameters (Å, °) and volume (Å^3) parametrized by second-order polynomials (see text)*

	R ($\times 10^{-3}$)
$a = 16.223 - 0.0165P + 0.00032P^2$	0.64
$b = 8.436 - 0.0215P + 0.00026P^2$	1.1
$c = 13.105 - 0.0474P + 0.008P^2$	1.2
$\beta = 110.27 + 0.157P - 0.00276P^2$	0.3
$V = 1682.4 - 13.74P + 0.236P^2$	2.7

$R = \sum_{i=1}^{n} |x_{cal} - x_{exp}| / \sum_{i=1}^{n} x_{exp}$.

Table 4. *Unit-cell parameters and their relative variation [1 × 10^5 Pa and 12.9 × 10^5 kPa, 295 K (this work); 1 × 10^5 Pa, 15 K (Schultz et al., 1991)]*

	1 × 10^5 Pa 295 K	12.9 × 10^5 Pa	$\Delta x/x$ ($\times 10^{-2}$)	15 K	$\Delta x/x$ ($\times 10^2$)
a (Å)	16.23	16.06	−1.0	16.37	+0.9
b (Å)	8.44	8.19	−2.9	8.37	−0.8
c (Å)	13.11	12.64	−3.6	12.77	−2.6
β (°)	110.26	111.82	+1.4	111.40	+1.0
V (Å^3)	1685	1544	−8.4	1630	−3.3

also the pressure at which the gap between the one-dimensional sheet and two-dimensional hole pocket in the Fermi surface becomes zero (Lubczynski *et al.*, 1994).

The data in Table 2 also enable us to calculate the components of the compressibility tensor and hence the amplitudes, and directions of its principal components (k_1, k_2, k_3), as well as the volume compressibility (k_v). As with the linear compressibilties the amplitudes of the three principal compressibilities are very different, although it is interesting that the ratio between these remains almost constant with increasing pressure. Nevertheless, the amplitude of the largest component k_1 (480 kPa^{-1}) is not very great: it is comparable to that found in (TMTSF)$_2$ClO$_4$ [410 kPa^{-1} (Houbib, 1988)], but somewhat smaller than those of (TMTSF)$_2$PF$_6$ [610 kPa^{-1} (Gallois, Gaultier, Hauw, Lamcharfi & Filhol, 1986)] or α′-(BEDT-TTF)$_2$AuBr$_2$ [530 kPa^{-1} (Chasseau *et al.*, 1993)]. Again, like the linear compressibilities, the principal compressibilities also decrease linearly with pressure.

Due to the monoclinic symmetry of κ-(BEDT-TTF)$_2$Cu(NCS)$_2$, one principal direction of compressibility lies along the b axis while the other two lie in the ac plane, as shown in Fig. 2. One makes an angle of 33° to c and the other an angle of 13° with a. The three directions do not change with pressure, in contrast to α′-(BEDT-TTF)$_2$AuBr$_2$ (Chasseau *et al.*, 1993) and α′-(BEDT-TTF)$_2$Ag(CN)$_2$ (Guionneau *et al.*, 1995).

The bulk modulus $B = k_v^{-1}$ is an important quantity once it parametrizes the energy required to deform the system [$B = -V(dP/dV) = V(d^2U/dV^2)$, where U is the potential energy] and hence gives information about its rigidity. At ambient pressure B is 122 × 10^5 kPa,

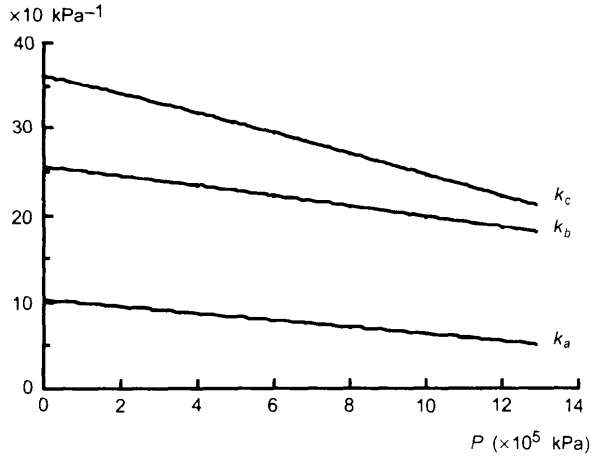

Fig. 1. Pressure dependence of the compressibility amplitudes of κ-(BEDT-TTF)$_2$Cu(NCS)$_2$ along the a, b and c axes.

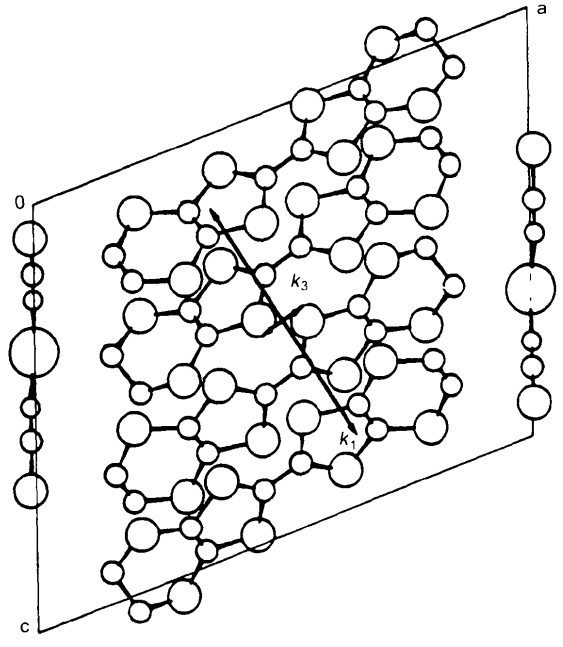

Fig. 2. Directions of principal compressibilities k_1 and k_3 with respect to the crystallographic axes.

very similar to that found for $(TMTSF)_2ClO_4$ (127×10^5 kPa; Houbib, 1988) but distinctly larger than those of $(TMTSF)_2PF_6$ (96×10^5 kPa; Gallois, Gaultier, Hauw, Lamcharfi & Filhol, 1986), α'-$(BEDT\text{-}TTF)_2AuBr_2$ (91×10^5 kPa; Chasseau *et al.*, 1993) and TTF-TCNQ (114 kbar; Filhol, 1985). With increasing pressure B increases, to reach the exceptionally high value of 191×10^5 kPa at 12×10^5 kPa, in contrast to the more one-dimensional conductor $(TMTSF)_2ClO_4$, for which B is almost invariant to pressure.

3.2. *Crystal structure at 1×10^5 Pa*

As expected, at 1×10^5 Pa the results of the structure determination are directly comparable to those of Urayama, Yamochi, Saito, Sato *et al.* (1988). Therefore, description is confined to those features bearing on the structure under pressure.*

The final R factors are smaller than those of Urayama, Yamochi, Saito, Sato *et al.* (1988), as are the e.s.d.'s of bond lengths and angles: The latter are of the order 0.006 and 0.009 Å on the S—C and C—C bonds, respectively, and 0.3 and 0.5° on C—S—C and S—C—C angles. Values of the bond lengths and angles in the two independent BEDT-TTF are given to three significant figures in Fig. 3 and those of the $Cu(NCS)_2^-$ in Fig. 4. With the exception of one ethylenic —S—C—C—S— group in each molecule, which is positionally disordered, the lengths of chemically equivalent bonds show only very small differences, the S—C clustering around the value 1.737 Å and the C=C bonds being 1.372 Å for the central bond of the BEDT-TTF and 1.347 Å for the external bonds. In the same way, equivalent bond angles show a dispersion of less than 1°, the largest differences being in the ordered ethylenic links, indicating that this is the most deformable part of the molecule. The positional disorder of the other —S—C—C—S— ethylene link in each molecule manifests itself by abnormally short bond lengths (1.3 Å instead of the expected 1.5 Å) and angles (C—C—S ≃ 130° instead of 115°). Furthermore, the thermal parameters of these atoms are between 9 and 13 Å^2 instead of ~4 Å^2. In contrast, the $Cu(NCS)_2^-$ moiety exhibits no significant disorder (Fig. 4).

3.3. *Crystal structure at 7.5×10^5 kPa*

The variation of the unit-cell parameters with pressure, described above, shows that there is no structural phase transition between 1×10^5 Pa and 12.9×10^5 kPa. Hence, the structure at 7.5×10^5 kPa was determined in monoclinic symmetry ($P2_1$). The cell parameters used to collect the data were determined in

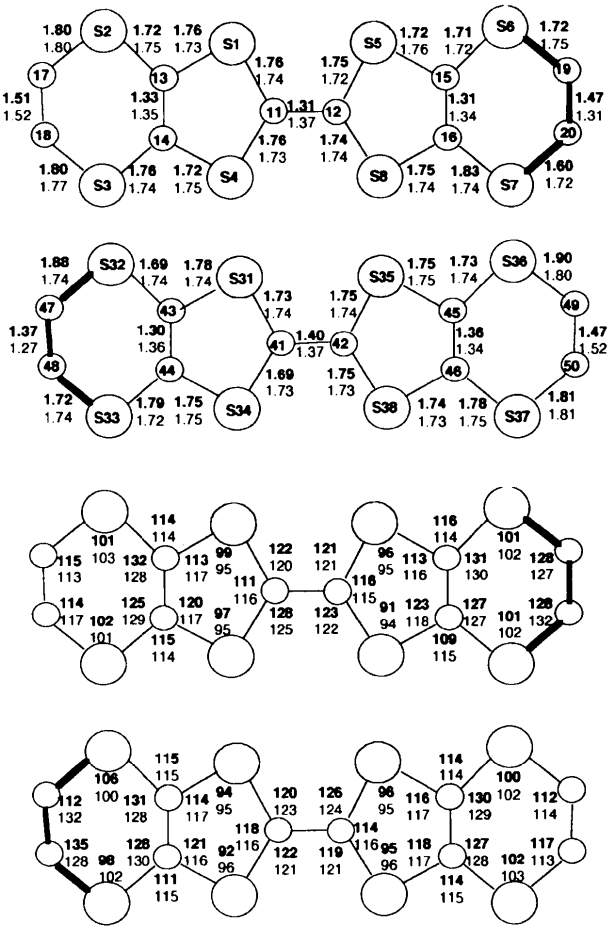

Fig. 3. Bond lengths and angles within the BEDT-TTF molecules in κ-$(BEDT\text{-}TTF)_2Cu(NCS)_2$ at 1×10^5 Pa and 7.5×10^5 kPa (bold). The bond lengths are rounded to 0.01 Å and the angles to 1°. The disordered ends of the molecules are indicated by thick lines.

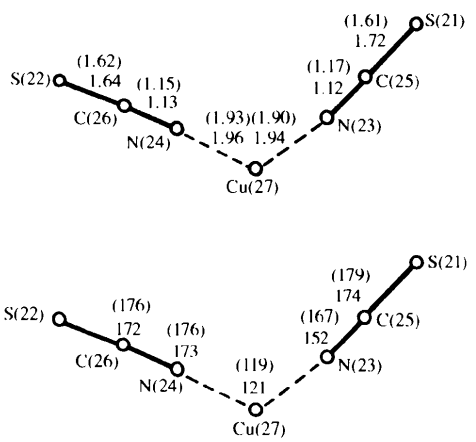

Fig. 4. Bond lengths and angles between the $Cu(NCS)_2^-$ moiety in κ-$(BEDT\text{-}TTF)_2Cu(NCS)_2$ at 1×10^5 Pa (in parentheses) and 7.5×10^5 kPa. Values are rounded as in Fig. 3.

* Lists of atomic coordinates, anisotropic displacement parameters and structure factors have been deposited with the IUCr (Reference: PA0300). Copies may be obtained through The Managing Editor, International Union of Crystallography, 5 Abbey Square, Chester CH1 2HU, England.

the same way as at 1×10^5 Pa and are listed in Table 1. Likewise, the data collection proceeded in the same fashion; although it should be noted that rather fewer reflections were measured. This was in part because ~12% of reflections were obscured by the framework of the pressure cell and in part because of the need to discard a certain number of reflections from the twinned crystal which could not be resolved into their components.

In the structure refinement the 'robust-resistant' weighting scheme (Prince, 1978) was adopted from the outset for all atomic positional and thermal parameters except for H atoms. Initial parameters were those of the ambient pressure refinement.* The final weighted R factor (Table 1) is comparable to that obtained at ambient pressure, although the e.s.d.'s are large because of the smaller number of reflections observed. The e.s.d.'s are in the region of 0.015 and 0.020 Å for S—C and C—C bonds and 0.7 and 1.0° for the C—S—C and S—C—C bond angles.

An immediate conclusion of importance for the physical behaviour is that the positional disorder found at one end of each BEDT-TTF molecule at 1×10^5 Pa is still present at 7.5×10^5kPa, as may be seen by comparing the change in the thermal parameters of these atoms. Thus, in BEDT-TTF (1) the mean values of B_{eq} for C(19) and C(20) are reduced by ~4 Å^2, the C(19)—C(20) distance increasing from 1.31 to 1.47 Å from 1×10^5 Pa to 7.5×10^5 kPa. In contrast, the mean values of B for the corresponding atoms C(48) and C(47) in BEDT-TTF (2) remain high and unaltered and the C—C distance remains low (1.37 compared with 1.27 Å at 1×10^5 Pa).

Both molecular cations appear to be 'stretched' at 7.5×10^5 kPa, as may be seen from the bond angles in the fulvalene rings, which are distorted by 10° in one molecule and 7° in the other. However, the mean value of S—C distances remains at 1.74 Å in both molecules, the same as at 1×10^5 Pa. The most significant finding in terms of the variation of the electronic structure with pressure is a shortening of the C=C bonds in BEDT-TTF (1) (external bonds from 1.35 to 1.32 Å and central bond from 1.37 to 1.31 Å), while in BEDT-TTF (2) the central C=C bond lengthens from 1.37 to 1.40 Å, although the mean of the two external C=C bond lengths remains unchanged. Deviation of the molecules from planarity is similar to that at 1×10^5 Pa.

As far as the Cu(NCS)$_2$ unit is concerned, pressure has little effect on the bond lengths and angles of the NCS$^-$ that forms part of a polymeric chain by being bound to Cu atoms at both ends. However, the effect on the NCS$^-$ that is only bound to Cu at one end is quite marked (Fig. 5): the N—C—S angle decreases by 5° and the N—C distance by 0.04 Å, while the S—C distance increases by 0.10 Å. As a result the arrangement of the ligands about the Cu is strongly modified, with the C—N—Cu angle falling from 167 to 152° and the two N—Cu distances each increasing by 0.03 Å. On the other hand, the N—Cu—N angle only increases by 2°.

Turning to the intermolecular interactions, the arrangement of BEDT-TTF molecules at 7.5×10^5 kPa is closely similar to that found at 1×10^5 Pa, because the symmetry constraints remain those of the $P2_1$ space group. Nevertheless, there are important changes in intermolecular distances and angles. The long axes of the BEDT-TTF lie along the a direction and the molecules form dimeric units. To describe the different intra- and intermolecular interactions between neighbouring BEDT-TTF, we label the ions with coordinates x, y, z as A, B and those related by a screw axis, with coordinates $-x+1, y+\frac{1}{2}, -z+1$ as Ā, B̄. Each ion has six neighbours, one (intradimer) with a normal interaction, labelled S, and five with transverse interactions, labelled I_i. A schematic view of the arrangement is shown in Fig. 6. The totality of these interactions is of course important in determining the band structure, established through overlap of the p_z orbitals of C and S. The S···S interactions are parametrized conveniently in terms of the distance d_{ij} and the angle φ that the vector d makes with the molecular plane. Table 5 lists the values of d_{ij} and φ_{ij} observed at 1×10^5 Pa and 7.5×10^5kPa. As far as the intradimer overlap is concerned, it can be parametrized by three variables; the interplanar distance d, the transverse displacement Δt and the longitudinal displacement Δl, the latter being defined

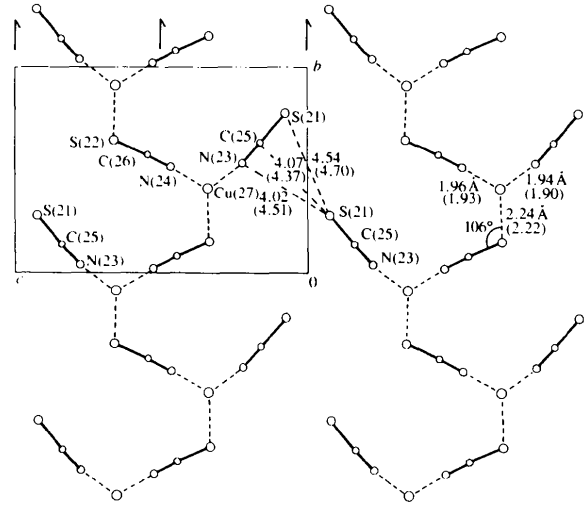

Fig. 5. Intermolecular bond lengths and angles between Cu(NCS)$_2^-$ in κ-(BEDT-TTF)$_2$Cu(NCS)$_2$ at 1×10^5 Pa (in parentheses) and 7.5×10^5 kPa, rounded as in Figs. 3 and 4.

* See deposition footnote on p. 163.

as the displacement of the centres of the molecules perpendicular and parallel to the long molecular axis. The following values were found:

1×10^5 Pa	d (Å)	3.39	Δt (Å)	0.06	Δl (Å)	1.78
7.5×10^5 kPa		3.31		0.06		1.72

Clearly the intradimer interaction S, already strong at 1×10^5 Pa, is further reinforced by pressure. With regard to the other interactions I_i, we find the S···S distances decrease by an average of ~0.09 Å (Table 5) and in the cases of I_2 and I_4, two additional S···S contacts less than 4 Å appear. Hence, we expect those interactions to be considerably reinforced.

3.4. *Effect of pressure on the electronic structure*

Having determined the crystal structure at 7.5×10^5 kPa, the effect of pressure on the electronic band structure can now be determined by evaluating the transfer integrals which express the intermolecular electronic coupling. The latter were calculated within the framework of the Extended Hückel Model (EHM; Hoffmann, 1963) from the diatomic overlap integrals and atomic ionization energies. The overlap integrals are a function, not only of the distance between the atoms concerned, but also (since we are concerned with p_z orbitals) of the angle made by the interatomic vector with the molecular plane. To calculate the transfer integrals the method of 'dimer-splitting' (Ducasse *et al.*, 1986) was employed: the coefficients of the highest occupied molecular orbital (HOMO) are calculated by EHM using 3*s*, 3*p*, 3*d* on S, 2*s*, 2*p* on C and 1*s* on H. The signs of the transfer integrals are negative when the interaction is of π-type and positive when it is σ. Small

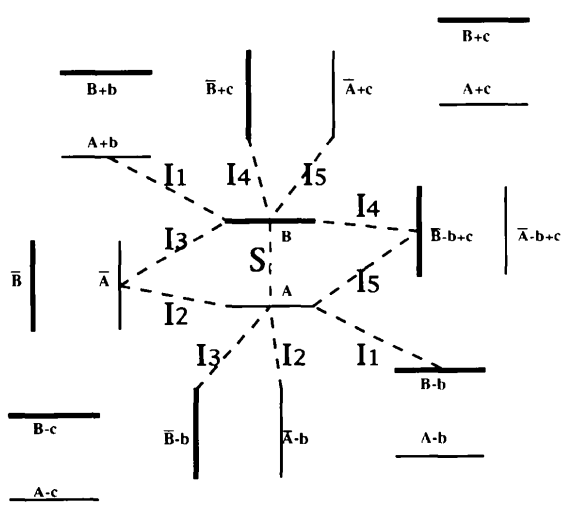

Fig. 6. Intra- (S) and interdimer (I_i) interactions between BEDT-TTF; A and B label the independent cations and Ā and B̄ label those related by the screw axis.

Table 5. *Intermolecular S···S interactions between BEDT-TTF molecules*

The atom-numbering scheme is that of Fig. 3; d_{ij} is the distance between *S* and φ_{ij}, the angle between this vector and the mean plane. for each quantity the first column is the value at 1×10^5 Pa and the second at 7.5×10^5 kPa.

Interaction	Dimer	s_i	s_j	d_{ij} (Å)		$\langle d_{ij} \rangle$	φ_{ij} (°)	
		1	31	3.83	3.75		63.4	63.4
		4	34	3.84	3.76		61.3	61.3
		4	33	3.93	3.79		73.8	73.8
S		5	35	3.77	3.77	3.73	60.6	60.6
	A,B	5	31	3.64	3.54	(3.81)	66.8	66.8
		6	36		3.96			73.3
		6	35	3.84	3.73		73.3	73.3
		8	38	3.91	3.84		64.1	64.1
		8	34	3.74	3.65		67.2	67.2
		1	33	3.56	3.50		−37.7	−37.0
I_1	A, B − b	2	33	3.55	3.47	3.46	−37.2	−38.7
	(B, A + b)	6	38	3.54	3.43	(3.54)	−38.4	−38.1
		6	37	3.51	3.43		−36.5	−37.6
		1	4	3.82	3.67		−70.9	−70.8
I_2	A, Ā − b	2	7		3.98	3.69		−55.0
	(A, Ā)	2	8	3.76	3.64	(3.78)	−71.6	−71.7
		5	3	3.67	3.62		−73.0	−72.1
		6	3	3.86	3.83		−53.8	−53.5
	A, B̄ − b	3	38	3.82	3.78		−69.2	−70.3
I_3	(B, Ā)	4	34	3.79	3.67	3.65	−69.9	−71.6
		8	33	3.69	3.49	(3.75)	−59.4	−60.8
		38	35	3.86	3.73		68.6	67.8
		38	31		3.97			58.3
	B, B̄ + c	37	32	3.79	3.71		58.0	57.3
I_4	(B, B̄ − b + c)	37	31	3.71	3.63	3.66	69.8	68.9
		34	36	3.68	3.60	(3.75)	70.9	70.0
		33	36	3.70	3.64		56.4	55.6
	B, Ā + c	36	1	3.78	3.79		73.2	74.7
I_5	(A, B̄ − b + c)	35	5	3.77	3.64	3.62	73.7	75.4
		31	6	3.58	3.43	(3.71)	63.4	64.9

corrections are introduced to take account of the deviation of the BEDT-TTF from planarity.

Values of the transfer integrals calculated from the structures determined at 1×10^5 Pa and 7.5×10^5 kPa are indicated in Fig. 6. At both pressures the integrals are all of bonding type and all increase with pressure (Table 6 also summarizes the transfer integrals calculated from positional parameters determined by us and other workers at various temperatures). That within the dimer is distinctly smaller than those found in the ambient pressure superconductor $(TMTSF)_2ClO_4$ (257 and 228 meV), but it increases by 23% up to 7.5×10^5 kPa, a much greater increase than that found for $(TMTSF)_2ClO_4$ at the same pressure (7%). As one might anticipate from the changes in interatomic distances, I_2 and I_4 increase by 30–40% while I_1, I_3 and I_5 only increase 7–11%. In all, therefore, the hierarchy of interactions is modified by pressure.

In view of the difference in the behaviour of the unit-cell parameters at high pressure and at low temperature, summarized in Table 4, it is of interest to calculate the transfer integrals from a low-temperature crystal structure. For this purpose we have used the positional

Table 6. *Transfer integrals (meV) calculated using atomic coordinates of (a) Schultz et al. (1991), (b) Urayama, Yamochi, Saito, Sato et al. (1988) and (c) of this present work for various temperatures and pressures ($c_1 = 1 \times 10^5$ Pa; $c_2 = 7.5 \times 10^5$ kPa)*

t (meV)	300 K (*a*)	300 K (*b*)	300 K (c_1)	118 K (*a*)	104 K (*b*)	15 K (*a*)	300 K (c_2)
S	129	134	136	148	150	142	162
I_1	49	50	50	44	44	45	54
I_2	45	41	41	55	48	61	58
I_3	29	27	27	21	25	17	30
I_4	45	47	48	49	55	55	62
I_5	25	28	28	25	22	30	30

parameters of Urayama, Yamochi, Saito, Sato *et al.*, (1988), 104 K, and Schultz *et al.* (1991), 118 and 15 K. While S, I_1 and I_4 increase, I_1, I_3 and I_5 actually diminish, as a result of the increase in a with decreasing temperature.

From the transfer integrals in Fig. 6 the electronic band structure can be evaluated. Fig. 7 shows the resulting energy dispersion curves and Fermi surfaces at 1×10^5 Pa and 7.5×10^5 kPa. In this figure the Brillouin zone centre (0,0) is labelled Γ and the Y, Z and M points are $(\pi/b, 0)$, $(0, \pi/c)$ and $(\pi/b, \pi/c)$, respectively. The four energy bands correspond to the four BEDT-TTF molecules in the unit cell, each represented by its HOMO. Overall, the curves are quite similar, although, in general, the 7.5×10^5 kPa ones lie at higher energy, the more so for the upper pair of levels. Indeed, the upper bands are displayed about the same amount in all the directions, which is not the case for the lower ones. Thus, between M and Z, and M and Γ the two lower bands are degenerate at ambient pressure, but the degeneracy is removed at 7.5×10^5 kPa. As expected, the total band width measured at the Γ point increases with pressure, since it is directly related to the transfer integrals, while for the same reason the Fermi level also increases from 127 to 210 meV. The latter difference is certainly significant given the value of kT at room temperature (~27 meV). Finally, the Fermi surface remains closed at 7.5×10^5 kPa, as expected of a two-dimensional system, but is shifted in an isotropic manner towards the edges of the Brillouin zone. Its area is reduced from 16% of the total surface at 1×10^5 Pa to 14% at high pressure, contrary to what is found at low temperature (Lubczynski *et al.*, 1994).

4. Conclusion

We have measured the magnitudes and directions of the principal components of the isothermal compressibility tensor of the superconducting molecular charge-transfer salt κ-(BEDT-TTF)$_2$Cu(NCS)$_2$ at 295 K and at pressures up to 12.9×10^5 kPa. The three directions do not vary with respect to the crystal axes, but the magnitudes decrease almost linearly with increasing pressure. Oshima *et al.* (1988) made an estimate of the linear compressibility in the *bc* plane from the pressure dependence of the period of the Schubnikov de Haas oscillations in the magnetoresistance. They found a value of 5×10^2 kPa^{-1}, which should be compared with 2.5×10^2 kPa^{-1} from our experiments. Furthermore, Toyota & Sasaki (1990) studied the effect of pressure on the band structure of κ-(BEDT-TTF)$_2$Cu(NCS)$_2$ to try to explain the sensitivity of T_c to pressure. In their model the conduction band is split into two sub-bands disposed symmetrically about the Fermi level as a result of inter-site Coulomb interactions. Pressure widens these bands and hence reduces the gap. Our experiments indicate that the values that Toyota and Sasaki used in their calculation were in fact quite reasonable estimates.

The directions of compressibility are determined by the relative sizes of the intra- and intermolecular

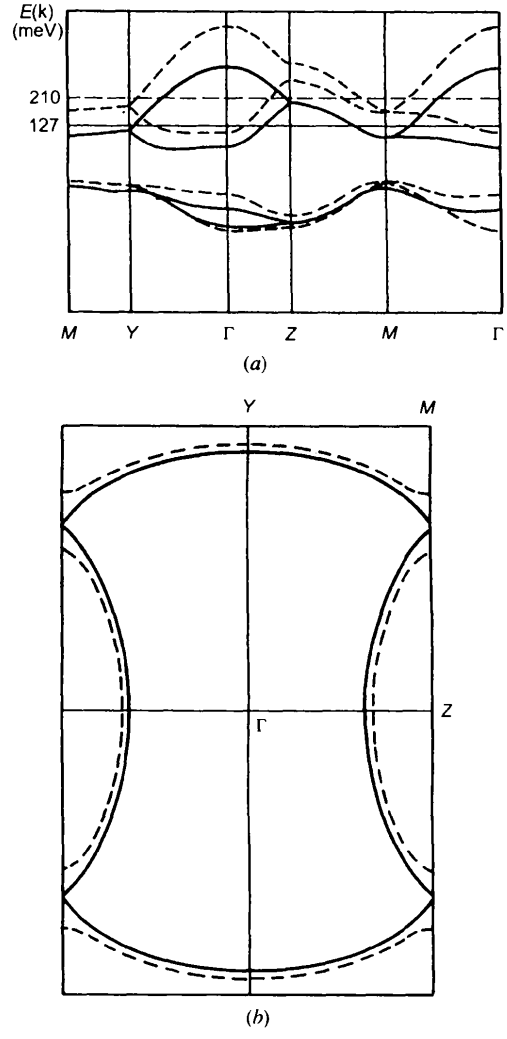

Fig. 7. (*a*) Band structure and (*b*) Fermi surface of κ-(BEDT-TTF)$_2$Cu(NCS)$_2$ at 1×10^5 Pa (full lines) and 7.5×10^5 kPa (dashed lines).

volumes, although given the complexity of the structure interpretation of the tensor is not straightforward. Nevertheless, certain conclusions may be drawn. The structure is constituted from BEDT-TTF dimers and polymeric $Cu(NCS)_2$ chains with neighbouring dimers orthogonal to one another: the largest compressibility k_1 is in the mean direction of the interaction between perpendicular dimers, while k_2 (which has an intermediate value) is in the mean direction of the interaction between parallel next-nearest neighbour dimers. Finally, the smallest compressibility k_3 lies parallel to the long axis of the BEDT-TTF molecular ions, *i.e.* in the direction in which the electron density is greatest.

As far as the crystal structure is concerned, the most significant result is that it does not change with pressure in a manner equivalent to that brought about by lowering the temperature. This is important in assessing the effect of temperature and pressure in the conductivity.

We thank SERC (UK), CNRS (France), NATO and the British Council for support, H. Mori and T. Mori for band structure data and atomic coordinates, and J. M. Williams for atomic coordinates.

References

Caulfield, J., Lubczynski, W., Pratt, F. L., Singleton, J., Ko, D. Y, K., Hayes, W., Kurmoo, M. & Day, P. (1994). *J. Phys. Condens. Matter*, **6**, 2911–2924.

Chasseau, D., Gaultier, J., Bravic, G., Ducasse, L., Kurmoo, M. & Day, P. (1993). *Proc. R. Soc. A*, **442**, 207–219.

Chasseau, D., Gaultier, J., Rahal, M., Ducasse, L., Kurmoo, M. & Day, P. (1991). *Synth. Met.* **41/43**, 2039–2042.

Cromer, D. T. & Mann, J. B. (1968). *Acta Cryst.* A**24**, 321–324.

Cromer, D. T. & Waber, J. T. (1974). *International Tables for X-ray Crystallography*, Vol. IV, Table 2.2A, pp. 149–160. Birmingham: Kynoch Press. (Present distributor Kluwer Academic Publishers, Dordrecht.)

Ducasse, L., Abderrabba, M., Hoarau, J., Pesquer, M., Gallois, B. & Gaultier, J. (1986). *J. Phys. C*, **19**, 3805–3820.

Emge, T. J., Leung, P. C. W., Beno, M. A., Wang, H. H., Firestone, M. A., Webb, K. S., Carlson, K. D. & Williams, J. M. (1986). *Mol. Cryst. Liq. Cryst.* **132**, 363–383.

Filhol, A. (1985). Thesis. University of Bordeaux, France.

Fujii, H., Kajita, K., Kawada, K., Nishio, Y., Kobayashi, H., Kobayashi, A. & Kato, R. (1993). *Synth. Met.* **55/57**, 2939–2945.

Gallois, B., Gaultier, J., Hauw, C., Lamcharfi, T. & Filhol, A. (1986). *Acta Cryst.* B**42**, 564–575.

Guionneau, P., Rahal, M., Bravic, G., Gaultier, J., Mellado, J. M., Chasseau, D., Ducasse, L., Kurmoo, M. & Day, P. (1995). *J. Mater. Chem.* **5**, 1639–1645.

Hoffmann, R. (1963). *J. Chem. Phys.* **39**, 1397–1412.

Houbib, H. (1988). Thesis no. 235. Univeristy of Bordeaux I, France.

Kang, W., Jerome, D., Lenoir, C. & Batail, P. (1990). *J. Phys. Condens. Matter*, **2**, 1665–1668.

Larsen, J. & Lenoir, C. (1988). *Synthesis*, **2**, 134.

Loumrhari, H. (1983). Thesis no. 1864. University of Bordeaux, France.

Lubczynski, W., Caulfield, J., Pratt, F. L., Singleton, J., Hayes, W., Kurmoo, M. & Day, P. (1994). *Physica B*, **210**, 483–486.

Oshima, K., Mori, T., Inokuchi, H., Urayama, H., Yamochi, H. & Saito, G. (1988). *Synth. Met.* **27**, A165–A170.

Parker, I. D., Friend, R. H., Kurmoo, M., Day, P., Lenoir, C. & Batail, P. (1989). *J. Phys. Condens. Matter*, **1**, 4479–4482.

Prince, E. (1978). *Am. Crystallog. Prog. Abstr. Ser.* **2**, 37.

Schirber, J. E., Venturini, E. L., Kini, A. M., Wang, H. H., Whitworth, J. R. & Williams, J. M. (1988). *Physica C*, **152**, 157–158.

Schultz, A. J., Beno, M. A., Wang, H. H., Kini, A. M., Williams, J. M. & Whangbo, M. H. (1991). *J. Solid State Chem.* **94**, 352–361.

Tokumoto, M., Murata, K., Bando, H., Anzai, H., Saito, G., Kajimura, K. & Ishiguro, T. (1985). *Solid State Commun.* **54**, 1031–1034.

Tokumoto, M., Murata, K., Kinoshita, N., Yamaji, K., Anzai, H., Tanaka, Y., Hayakawa, Y., Nagasaka, K. & Sugawara, Y. (1990). *Mol. Cryst. Liq. Cryst.* **181**, 295–304.

Toyota, N. & Sasaki, T. (1990). *Solid State Commun.* **74**, 361–365.

Urayama, H., Yamochi, H., Saito, G., Nozawa, K., Sugano, T., Kinoshita, M., Sato, S., Oshima, K., Kawamoto, A. & Tanaka, J. (1988). *Chem. Lett.* pp. 55–58.

Urayama, H., Yamochi, H., Saito, G., Sato, S., Kawamoto, A., Tanaka, J., Mori, T., Maruyama, Y. & Inokuchi, H. (1988). *Chem. Lett.* pp. 463–466.

Williams, J. M., Ferraro, J. R., Thorn, R. J., Carlson, K. D., Geiser, U., Wang, H. H., Kini, A. M. & Whangbo, M. H. (1992). *Organic Superconductors (Including Fullerenes) Synthesis, Structure, Properties and Theory*. New Jersey: Prentice Hall.

Yagubskii, E. B., Shchegolev, I. F., Laukhin, V. N., Kononovich, P. A., Kartsovnik, M. V., Zvarykina, A. V. & Buravov, L. (1984). *JETP Lett.* **39**, 12–16.